Losses in an Optimized 8-pole Radial AMB for Long Term Flywheel Energy Storage

L.Bakay*, M. Dubois*, P. Viarouge*, and J. Ruel**
* E lectrical Engineering Department, LEEPCI, Laval University, QC G1V 0A6, CANADA
** Mechanical Engineering Department, Design Bureau, Laval University, QC G1V 0A6, CANADA

Abstract-- **In this paper, we will study the effect of losses (non including losses in the power electronic) of an optimized eight pole radial AMB on the discharge time of a no-load Long Term Flywheel Energy Storage (LTFES). Load capacity is the main parameter of an Active Magnetic Bearings (AMB) design. This parameter has to take into account the external disturbance force which may be constant, synchronous with the rotor angular velocity or completely general. To relatively simplify this study, we restricted the effect of external disturbance to a constant unbalance force only. The latter plays a high part on the size of bearing system. Before optimizing the AMB design, we have built and validated an Excel theoretical model with 2-D Finite Element Method (FEM). Several optimizations have been made in order to seek the minimum of both copper and iron losses we could obtain for a given load capacity. Then, evolution of losses functions of angular velocity speed of rotor has been drawn. Flywheel discharge time has been computed to pass from 9000 rpm to 4500 rpm and evolution of this time versus mass of AMB has been shown for different values of unbalance forces**.

Index Terms-- **Active magnetic bearing, Long Term Flywheel Energy Storage, losses, optimization**

I. INTRODUCTION

Nowadays, Flywheels Energy Storage (FES) is one of most attractive solutions for energy storage in both short and long term because they can be designed to have more than 100,000 charge and discharge cycles [1]. The FES's found on the market or studied in past literature are usually operated for the short discharge periods. This paper investigates Low loss FES with a long discharge time, namely 24 hours. To ensure low losses in this kind of system, especially in standby, active magnetic bearings are used owing to their absence of any contact between the rotating and non-rotating parts of the flywheel. Magnetic bearings are therefore free of lubricant and wear. Although they eliminate the friction losses, AMBs introduce copper and magnetic losses. To stabilize the FES system in its five degrees of freedom, two radial bearings and one axial bearing (either passive or active) are often used whereas the sixth degree of freedom is controlled by a motor/generator drive [2]. In this paper the FES uses two radial active bearings and one passive bearing.

The principle of a radial AMB is to radially act to keep the rotor centered. In the case of an active magnetic bearings, a position sensor must be associated to the electromechanical device, thereafter the position measured by the sensor is compared with a reference position by a feedback operation and the result is sent into a position controller and, according to the result obtained, an amplifier sets the desired current to the coil in order to generate a radial force which maintains the rotor centered.

In the Long Term Flywheel Energy Storage of fig.1, loss minimization of the overall system is required. Therefore, the losses of each component (i.e. motor/generator, flywheel, magnetic bearing...etc.) of the system must be minimized. In this paper, we focus on the radial AMB losses and their effects on the flywheel discharge time. Also, friction aerodynamic losses are not taken into account, neither are the losses in the power electronics device needed to drive the bearing (fig.2). Only the electromagnetic losses are considered.

Firstly, we design and optimize an AMB according to these requirements. Secondly we compute both the magnetic and copper losses and then, we calculate the flywheel discharge time for given maximum and minimum angular velocity speeds of the rotor. The evolution of this time versus the mass of the AMB is shown for different values of unbalance forces.

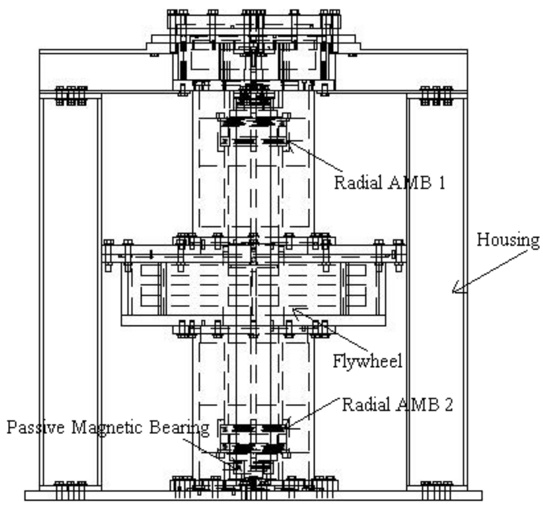

Fig.1: Flywheel assembly

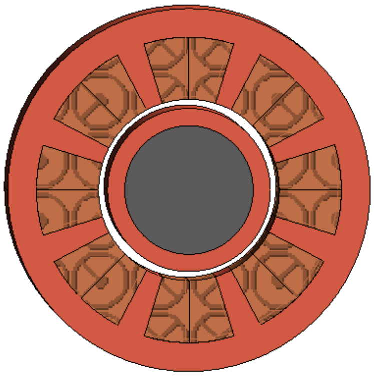

Fig. 2: Radial AMB geometry

II. FLYWHEEL UNBALANCE FORCE MODEL

A rotating mass is subject to external forces, which may be constant, either synchronous or non-synchronous with the rotor angular velocity or completely general — earth-quake for instance. To simplify this present work, we restricted the effect of external disturbance to a constant unbalance force only. Whatever balancing quality is specified for a rotating element, some residual unbalance will be present at start and further unbalance may develop in service. This unbalance gives rise to synchronous forces that may provide very important excitation of a rotor-bearing system [3]. These radial forces determine the force requirement of radial AMB. Therefore, AMB electromechanical devices have to take into account the flux flowing in the AMB core due to the response of the amplifier, with respect to disturbance. Fig. 3 shows the principle of unbalance force generation, wherein the rotor is considered as perfectly symmetrical but having an additional mass m_e (expressed in kg) at a radius of ε (m) with an angle Ωt, where Ω (rad/s) is the rotational angular speed of the rotor. The radial force is projected on the x-y axes as defined by [4].

$$F_x = m_e \varepsilon \Omega^2 \cdot Cos(\Omega t) \qquad F_y = m_e \varepsilon \Omega^2 \cdot Sin(\Omega t) \qquad (1)$$

The amplitude of these forces is proportional to the square of rotational speed. Generally, m_e and ε are unknown and depend on acceptable eccentricity of the center of gravity specific to the application. Denoting ε_{CG} the eccentricity of the center of gravity of the *whole* rotor

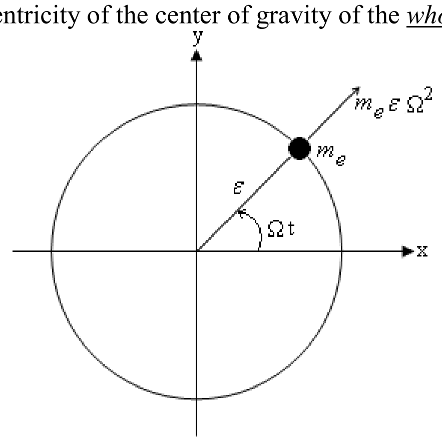

Fig. 3: Unbalance mass principle

TABLE I: Balance quality grade

Rotor types	Balance quality grade G (mm/s)
Cars wheel	40
Parts of agricultural machinery	16
Flywheels	6.3
Turbo-compressors	2.5
Spindles	0.4

of mass m, the unbalance force is then $F = m\varepsilon_{CG}\Omega^2$, where $m\varepsilon_{CG}$ corresponds to the rotor unbalance U(kg-m). Thus the unbalance force may be simplified as the product of unbalance U and the square of the rotation speed Ω.

$$F_{max} = U \cdot \Omega^2 \qquad U = \frac{G}{\Omega} \cdot m \qquad (2)$$

The G parameter is the balance quality grade. Typical values of the balancing grade G are given in [5]. For a flywheel, the typical value for G is 6.3 mm/s. It must be mentioned that although G is generally expressed in mm/s, for equations (2) to be consistent, calculations must be performed with G expressed in m/s. From eq. (2), it can also be observed that the balance quality grade G depends on the product of unbalance and the rotation speed. From (2), we can infer the maximum force F_{rmax} which acts on each radial AMB and which, with a security factor, will fix the design of the AMB.

$$F_{r\max} = \frac{U \cdot \Omega^2}{2} \qquad (3)$$

Some typical values of balancing grades G given by [5] are reported on table I.

A. Radial AMB geometry

In the AMB literature, we commonly find radial AMBs with three, four, six and eight poles. Knowing that the control of three, four or six AMB poles is more sophisticated because of the interaction of flux between the poles, the AMB choice depends on either the requirements or complexity of the application.

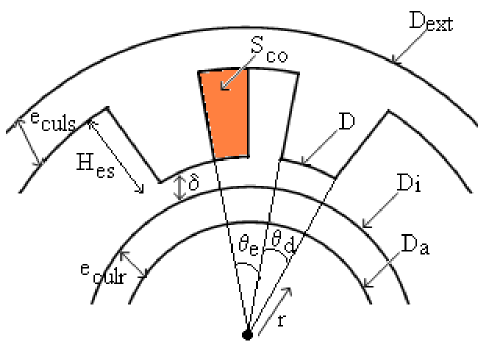

Fig. 4: Analysis model of Radial AMB

TABLE II: INPUT DATA OF RADIAL AMB

AMB maximum Outer diameter	Dext	270 mm
Number of poles	8	∅
Coils turn (for each electromagnet)	100	∅
Air gap	δ	1 mm
Flywheel shaft diameter	Da	100 mm
AMB maximum axial length	L	150 mm
Flywheel rotor mass	200	kg

Here, this study is restrained to eight-pole radial AMB geometry because it enables easy control of each electromagnet force separately to drive the four currents flowing in the electromagnets. Four power amplifiers are required as well.

In section B, the electromagnetic force is calculated and relationship between the latter and the geometric parameters such as tooth angle θ_d, inner diameter D and axial length L of the radial AMB is shown on the model of fig. 4 and expressed in (8).

D_{ext} and maximum axial length L which have been fixed from the flywheel housing size and others parameters are presented in Table II.

B. *Electromagnetic force computation*

Several magnetic force calculation methods are introduced in the literature. Among these methods, we can find the force calculation based on magnetic co-energy variation (4) which we used in this work.

$$\frac{\partial W'}{\partial \delta} = F_m \tag{4}$$

where W' is the co-energy of system, δ the air gap and F_m the electromagnetic force. For the purpose of computing energy, the inductance L_b of each electromagnet is calculated assuming that the magnetic circuit is linear and assuming the relative permeability of material much higher than air. Taking into account these assumptions, the inductance can be computed as shown in (5)

$$L_b = N^2 \cdot \frac{1}{2 \cdot \int_{Di/2}^{D/2} \frac{dr}{\mu_0 S(r)}} \tag{5}$$

where N is the number of turns of the winding and S(r) the cross-section of the flux path in the air gap from the tooth to the rotor laminations.

$$S(r) = r \cdot \theta_d \cdot L \tag{6}$$

The energy and co-energy of the system are equal if we assume that the AMB operates in the linear region of the laminations B(H) curve. Pole pair energy is essentially located in the coil inductance and can be written as (7), where *i* is the current in the electromagnet.

$$W_m = \frac{1}{2} L_b i^2 = N^2 \cdot \mu_0 \theta_d L \cdot \ln\left(\frac{D}{D_i}\right)^{-1} i^2 \tag{7}$$

Relationships (4) and (7) for each electromagnet become:

$$F_m = J^2 \cdot S_{co}^2 \cdot \mu_0 \theta_d L \cdot \frac{d}{d\delta}\left(\ln\left(\frac{D}{D_i}\right)^{-1}\right) = k \cdot J^2 \tag{8}$$

where J the current density and k is a factor taking into account the dimensions of the AMB.

$$k \approx \alpha \cdot \frac{S_{co}{}^2 \cdot \mu_0 \cdot L \cdot (D/2) \cdot \theta_d}{\delta^2} Cos\left(\pi/8\right) \tag{9}$$

In order to take into account the effective section of winding, a winding filling factor α is introduced.

The bearing current i can be defined as being the sum of a constant current I_0 which ensures stiffness of the rotor and a sinusoidal current Δi allowing compensation of the peak value of unbalance force around the operating point I_0. Knowing that J_0 and ΔJ_{max} are respectively the current densities of current I_0 and Δi — which are related by Sco —, the radial force Fm of AMB becomes:

$$F_m = k \cdot (J_0 + \Delta J_{max})^2 \tag{10}$$

Defining the maximum value of the magnetic flux density *Bmax* at the limit of linearity of B-H curve ensures quasi-linear magnetic properties in the entire operating range.

Moreover, the optimal operating point B_0 due to I_0 of the radial AMB is defined as the half value of the maximum magnetic flux density as shown in figure 5.

C. *Loss computation*

While there is no mechanical friction between the stator and rotor in magnetic bearings, copper, iron and aerodynamic losses must be considered. These losses, which heat up the rotor, will slow down the flywheel,

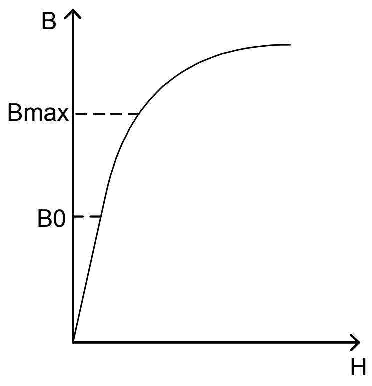

Fig 5: B-H material curve

given that the power used to control the AMB comes from the energy stored in the flywheel.

1) Copper Losses

Copper losses P_{co} depends on copper resistivity ρ_{co}, copper volume V_{co} and current (both pre-magnetization and disturbance current) density J as expressed in (11). They are essentially located on the stator of AMB.

$$P_{co} = \rho_{co} \cdot V_{co} \cdot \left(J_0 + \frac{\Delta J_{\max}}{\sqrt{2}} \right)^2 \quad (11)$$

Because of the current density J_0, constant losses appear even in the absence of any disturbance.

2) Iron losses in AMB NSSN configuration

The iron losses P_{iron} are due to a variety of mechanisms related to the fluctuating magnetic field and are located in both the stator and the rotor. In prior work, iron losses in the stator have been neglected [6] but in the case of a long term energy storage application, these have to be taken into account. To reduce aerodynamic losses resulting from aerodynamic drag, vacuum housing is used. Usually, iron losses are divided into two components, eddy currents losses P_{ed} and hysteresis losses P_h. To reduce eddy currents losses, laminated materials are often used.

$$P_{iron} = P_h + P_{ed} \quad (12)$$

According to the Steinmetz relationship, measurement and computation of core losses density for sinusoidal flux density repartition of magnitude B and frequency f is modeled in (13).

$$p_{iron} = k_h B^n f + k_{ed} B^2 f^2 \quad (13)$$

The coefficients k_h, k_{ed} and n depend on the thickness and the conductivity of the used laminated material.

a) Iron losses assessment

Figure 6 presents the flux density through the AMB.

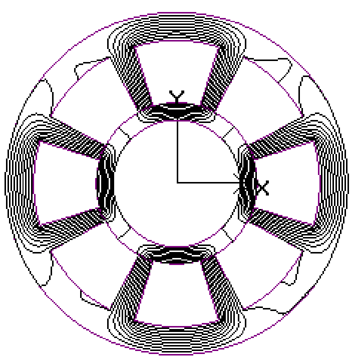

Fig 6: AMB Flux repartition

(1) Iron losses in stator

Given that the unbalance is sinusoidal, the current response — disturbance current — delivered by the amplifier is assumed to be sinusoidal. In absence of any disturbance current, only the bias current flows in the coils, which does not generate iron losses. However, in presence of unbalance force, iron losses occur in stator due to presence of disturbance current. For each part of the stator, namely yoke and teeth, iron losses are computed according to (12) and (13). In the case of iron losses in stator, the electric frequency f of the flux density in (13) is the same as the frequency of the unbalance.

(2) Iron losses in rotor

While the rotor is running, even if the disturbance current is nil, the variation of flux density B in the airgap due to the bias flux flowing in rotor yoke trough the stator and airgap generates iron losses in the rotor. These iron losses are inferred from (12) and (13) as well. In these expressions, f is twice bigger than the mechanical frequency because two flux density periods are contained in a geometric period of rotor as discussed in [7].

III. AMB Optimization Results For Low Losses

A. Discharge time computation

Before computing the discharge time of a flywheel in standby mode, it is suitable to draw some curves such as Losses (fig. 7) and Loss Torque TL (fig. 8) versus rotor angular speed Ω. The latter allows solving the dynamic equation in order to present rotor angular speed evolution. Note that the figures 7, 8 and 9 are inferred from a same AMB design which is presented on table II, while the fig.10 presents four different designs.

Total losses in an AMB are the sum of both the magnetic losses and copper losses. At $\Omega = 0$, unbalance force and magnetic losses are null according to (2) and (13). In this case, the AMB does not need any compensation current and therefore, losses are essentially due to the copper losses (due to I_0). In the case of Long Term Energy Storage, this occurs either at start-up or in case of flywheel failure.

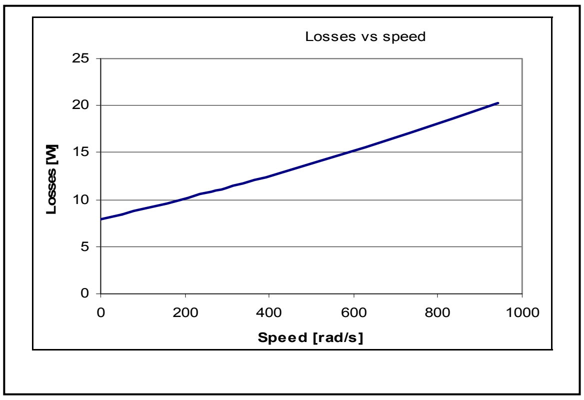

Fig 7: Radial AMB losses evolution

As flywheel supplies itself via motor/generator drive, at start-up AMBs need an external source of energy to keep the flywheel centered.

For this flywheel the speed operation ranges between 9000 RPM and 5000 RPM, and Fig.8 shows the evolution of the loss torque and its linear regression in that speed range

The linear regression form of loss torque is expressed as

$$T_L = A \cdot \Omega + B \quad (14)$$

where A is the slope and B the loss torque at $\Omega = 0$. From the dynamic equation, the torque assessment of both the flywheel and radial AMB can be written as (15), where J_f is the flywheel moment of inertia.

$$J_f \frac{d\Omega}{dt} + T_L = 0 \quad (15)$$

Expression for the flywheel speed (16) is the solution of equations (14) and (15).

$$\begin{cases} \Omega(t) = \left(\Omega(0) + \frac{B}{A} \right) \cdot e^{\frac{A}{J_f} t_f} - \frac{B}{A} \\ \Omega(0) = \Omega_{\max} \end{cases} \quad (16)$$

Parameters A and B are the results of linear regression of loss torque, which are calculated to have a best approximation of the loss torque curve.

The discharge time t_f is the time required for the flywheel, to see its speed decay from the maximum speed Ω_{max} to the minimum speed Ω_{min} taking into account the losses of the radial AMB only. Expression of that time is

$$t_f = \ln \left(\frac{\Omega_{\min} + \frac{B}{A}}{\Omega_{\max} + \frac{B}{A}} \right) \cdot \frac{J_f}{A} \quad (17)$$

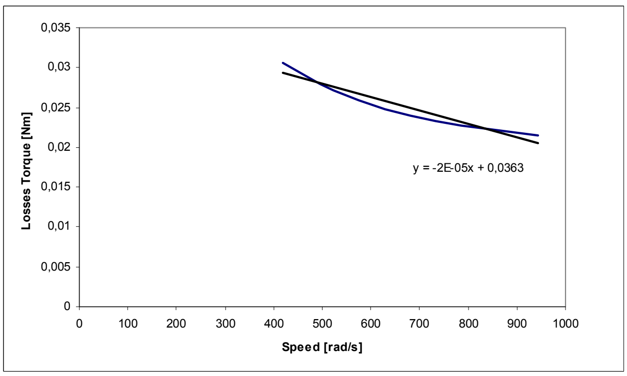

Fig 8: Radial AMB loss torque evolution

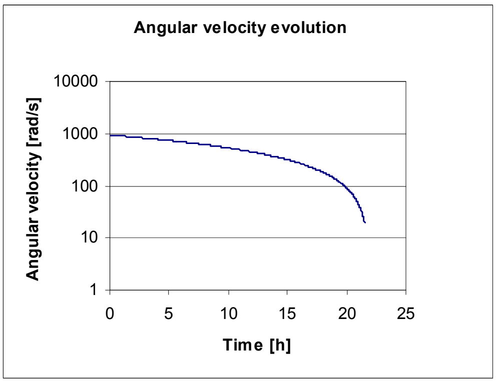

Fig 9: Flywheel speed decay (semi-log expression)

B. Optimization results

The discharge time expressed in (17) is the objective function in the radial AMB optimization. Discharge time being inversely proportional to AMB losses, the minimization of the losses will maximize t_f.

Fig.9 shows a semi-log flywheel speed decay function of t_f, which is derived from the same design used to plot figures 7 and 8. That curve can be divided in two parts, the straight line describing the low kinetic energy decay and a bowed part describing an important collapse of the flywheel energy. In case of a LTFES, it is important to operate in the straight zone

Fig. 10 presents the discharge time variation functions of AMB mass for some given unbalance force amplitudes. There, it is shown that for high discharge time i.e. low loss, AMB mass is smaller than in case of low discharge time.

Figure 11 shows the effect of the amplitude of unbalance (which balancing grade G = 6.3 mm/s) on both AMB mass and discharge time. When the amplitude of unbalance force increases, the AMB becomes bigger than in the case of lower amplitude. However, to provide a compensation force to overcome unbalance, the current flowing in the coil increases, generating important copper losses, which decrease the discharge time. Therefore, to obtain a long discharge time, it is important to minimize effect of unbalance, which will reduce AMB mass as well.

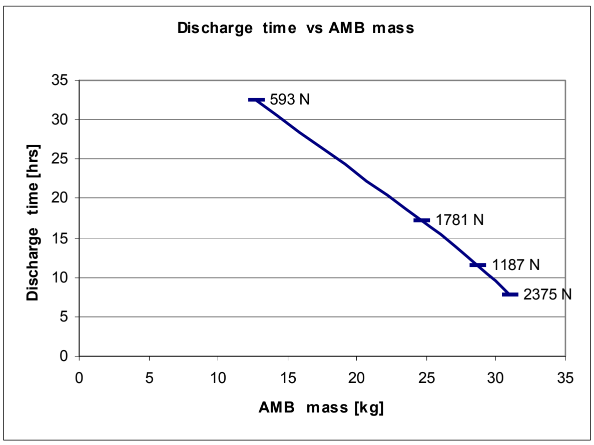

Fig 11: Discharge time versus AMB mass

IV. Conclusion

In order to quantify the losses induced by magnetic suspension in Long Term Flywheel Energy Storage, radial AMB design was presented. We have specially shown the rotor angular speed effect on the AMB losses and the AMB mass effect on the flywheel discharge time. It emerged that, to overcome unbalance force, radial AMB mass has to grow and therefore, flywheel discharge time decreases with AMB mass.

For an external unbalance force of 2375N, a radial AMB mass of 46.5kg (103 lbs) and an outer of 270mm, the discharge time is reported to slow down from 9000 rpm to 4500 rpm is 8.75h, which means important losses. This time is not acceptable for a Long Time Flywheel Energy Storage. Future work will be based on Homopolar Radial Magnetic Bearings biased by Permanent Magnet.

References

[1] A. Palazzolo, D.Pang, D.K. "Extreme Energy Density Flywheel Energy Storage System for Space Applications"

[2] G.Schweitzer, H. Bleuler and A.Traxler, "Active Magnetic Bearings" Vdf Hochschlverlag AG an der ETH Zürich, 1994.

[3] A.V. Ruddy "Rotor dynamics of turbo-machinery", The Glacier Metal Co.Ltd, Industrial Lubrication and Tribology, April 1984

[4] A.Chiba, T. Fukao, O. Ichikawa, M. Oshima, M. Takemoto and D.G Dorrell "Magnetic bearings and bearingless Drives" Newnes – Elvesier publications - 2005, ISBN 0 7506 5727 8.

[5] www.fr.schunk.com/schunk_files/attachments/Berechnung_Gesamtwuchtguete_EN_FR.pdf

[6] Habermann, "Fonction guidage en rotation, Paliers magnétiques" Techniques de l'Ingénieur. Génie Mécanique Vol. BD3 ,1984

[7] F.Matsumura and K.Hatake, "Relation between Magnetic Pole Arrangement and Magnetic Loss in Magnetic Bearing" in *Proc. 3rd Int. Symp.Magnetic Bearings*, July 1992, pp.274–283.